AIAA 90-0360
Unsteady and Quasi-Steady Vaporization of Spherical Droplet Clouds

M. Yang and M. Sichel
Univ. of Michigan
Ann Arbor, MI

28th Aerospace Sciences Meeting
January 8-11, 1990/Reno, Nevada

AIAA-90-0360

Unsteady and Quasi-Steady Vaporization of Spherical Droplet Clouds

Muh-Hsiung Yang and Martin Sichel

Department of Aerospace Engineering
The University of Michigan
Ann Arbor, Michigan 48109-2140

ABSTRACT

Group phenomena for droplets in a spray have often been analyzed on the basis of the quasi-steady assumption even though this assumption has not been completely justified. In this paper the applicability of the quasi-steady assumption to the vaporization of spherical droplet clouds is first analyzed qualitatively by considering the magnitudes of appropriate characteristic scales. Then the governing equations for the unsteady vaporization of a droplet cloud are formulated and solved by numerical methods. The numerical results indicate that cloud vaporization is inherently unsteady and consistent with the analysis of characteristic scales. The unsteady cloud vaporization nearly follows a "D-law" rather than the well "D^2-law" which governs the vaporization and combustion of liquid fuel droplets. Further it is found saturation conditions within the cloud cannot be uniquely determined as shown by the quasi-steady theory. However, the quasi-steady theory still provides a good prediction of cloud lifetime if the following two conditions are satisfied: (1) $\beta_0 \geq 1$, and (2) the existence of a thin vaporization layer or wave at the cloud edge.

Introduction

The collective behavior of liquid droplets in a practical spray usually results in a relatively cool, fuel-rich and air-deficient region in the spray interior, so that the behavior of droplets in a spray is significantly different from that of isolated droplets[1,2]. This group phenomenon is frequently analyzed by invoking the quasi-steady assumption for the regions within and outside the cloud, even though this assumption has not been justified rigorously[3,4]. The unsteady calculations of the group combustion of a very dilute droplet cloud recently carried out by Zhuang et al[5], have shown results different from the previous quasi-steady analyses. It is known that the success of the quasi-steady approximation in the single droplet theory is due to the large liquid-gas density ratio ($\bar{\rho}_d/\bar{\rho}_g$). However, the average density of the droplet cloud with a mass loading ratio $\beta_0 \approx O(1)$ is of the same order of magnitude as that of the ambient gas. The question of whether the quasi-steady assumption is valid for the vaporization of a spherical droplet cloud provides the subject of this study.

The unsteady vaporization in the interior of a saturated droplet cloud was first studied by Correa and Sichel[6,7] using asymptotic methods. The small parameter ε used in this asymptotic analysis is given by

$$\varepsilon = (2\pi \bar{n}_0 \bar{D}_{d0} \bar{R}_0^2)^{-1} = (\bar{\delta}/\bar{R}_0)^2 \qquad (1)$$

where $\bar{\delta} = (2\pi \bar{n}_0 \bar{D}_{d0})^{-1}$ was shown to be the thickness of a vaporization front at the outer surface of the spray cloud. (All symbols are defined in the nomenclature with overbars used for dimensional variables). The parameter ε resulting from the nondimensionalization of the governing equations is in fact the inverse of the group combustion number G which was proposed earlier by Chiu and his coworkers[3,8] as a parameter governing the group combustion phenomena. Practical sprays usually fall into the high G group combustion regime which is typified by a sheath or vaporization layer at the edge of the cloud. The relevance of the parameter G to practical sprays becomes apparent when G or ε is expressed in terms of the droplet mass loading ratio β_0:

$$G = \varepsilon^{-1} = 12 \frac{\bar{\rho}_g}{\bar{\rho}_d} \frac{\bar{R}_0^2}{\bar{D}_{d0}^2} \beta_0 \qquad (2)$$

For typical sprays with $\beta_0 \approx O(1)$, $\bar{\rho}_d/\bar{\rho}_g \approx 10^3$, $\bar{R}_0/\bar{D}_{d0} \approx O(10^3)$, then $G \approx O(10^4)$ and $\varepsilon \approx O(10^{-4})$. Correa and Sichel[6,7] have shown that in a saturated spherical cloud under these conditions vaporization occurs within a laminar vaporization layer or wave at the edge of the cloud propagating into the cloud, and that the cloud can be shown to behave as a large single droplet (see Fig. 1). The propagation speed of this vaporization front is a function of the cloud edge temperature and is given by[6,7]

$$\tilde{U}_w = \varepsilon \frac{\sqrt{6}\, \bar{R}_0 \bar{\lambda}}{(\bar{D}_{d0}/2)^2 \bar{\rho}_d \bar{C}_{p_g}} T_g^e \qquad (3)$$

where T_g^e represents the $O(\varepsilon^{1/2})$ term of an expansion of the dimensionless temperature at the cloud edge, i.e., $T^e = \varepsilon^{1/2} T_g^e + \varepsilon T_{g1}^e + \cdots\cdots$

The wave speed and hence cloud life time are therefore determined by the cloud edge temperature T_g^e. The edge temperature T_g^e needs to be determined by matching the solutions within and outside the cloud. In their analysis Correa and Sichel[6,7] applied the quasi-steady approximation to the ambient region located in the vicinity of the cloud and obtained a "D^2-law" for cloud vaporization analogous to that for single liquid droplets. The quasi-steady approximation is justified by the existence of the low-speed

vaporization wave which separates the the cloud into an inner quasi-steady and an outer, essentially unsteady region. As already indicated above,the quasi steady analysis works extremely well for single droplets, mainly because of the large value of $\bar{\rho}_d/\bar{\rho}_g$, the ratio of the liquid to the gas density; however, the ratio of the spray to the gas density is more likely of O(1). Hence, it is important to determine to what extent the quasi-steady assumption outside the cloud can be applied safely.

In the following the characteristic scales for evaluating the quasi-steady behavior outside the cloud are first discussed, and some important results obtained by Correa and Sichel are briefly reviewed. The fully unsteady governing equations for vaporizing spherical clouds are then formulated and solved by numerical methods. The comparison of the numerical results with the quasi-steady results is consistent with the analysis based on characteristic scales. It is shown that the quasi-steady analysis may over-predict the cloud edge temperature and under-predict the cloud lifetime unless $\beta_0 \geq O(1)$.

Characteristic Scales and Quasi-Steady Results

In the single droplet theory, the success of the quasi-steady assumption is due to the fact that the gas diffusion time across a distance of the order of the droplet diameter is small compared to the droplet lifetime. In analogy, it is of interest to compare the gas diffusion time across the cloud with the characteristic cloud lifetime determined by the quasi-steady theory [6,7], and the ratio of these times is given by:

$$\frac{\text{gas diffusion time across the cloud}}{\text{characteristic cloud life time}} = \frac{\bar{R}_0^2/\bar{a}_0}{\bar{R}_0/\bar{U}_w} = \left(\frac{1}{\beta_0}\frac{\sqrt{6}}{3}T_g^e\right) \qquad (4)$$

From Eq. (4) it appears that the quasi-steady assumption for the region outside the cloud will only be valid for $\beta_0 >> 1$ since $T_g^e \approx O(1)$. However, β_0 should not be too large (e.g. $\beta_0 < 10$) since the interaction between droplets has not been considered in Correa and Sichel's studies and will not be considered here. Therefore preliminary results which follow from Eq. (4) are:

If $\beta_0 \leq O(1)$, then diffusion velocity < wave velocity;
Ambient region is unsteady.

If $\beta_0 \geq O(1)$, then diffusion velocity > wave velocity;
Ambient region needs to be investigated. (5)

As already noted, the quasi-steady analysis was used by Correa and Sichel[6] to determine the cloud edge temperature which in turn determines the propagation speed of the vaporization layer. The quasi-steady analysis was assumed valid due to the low-speed and small thickness $\bar{\delta}$ of the vaporization layer which hinders the penetration of the heat from the ambient into the saturated cloud. The thickness $\bar{\delta}$ of the vaporization layer would thus appear to be the appropriate length scale in the quasi-steady analysis. Since $\bar{\delta}/\bar{R}_0 \approx O(\varepsilon^{1/2})$, the quasi-steady analysis therefore should only be valid in the region $R < r < R + O(\varepsilon^{1/2})$. The ratio of the gas diffusion time to the wave propagation time across the wave thickness can be written as

$$\frac{\text{gas diffusion time across the wave thickness}}{\text{propagation time across the wave thickness}} = \frac{\bar{\delta}^2/\bar{a}_0}{\bar{\delta}/\bar{U}_w} = \frac{\varepsilon^{1/2}}{\beta_0}\frac{\sqrt{6}}{3}T_g^e \qquad (6)$$

From Eqs. (4) and (6) it follows that the quasi-steady assumption will be valid both within the vaporization wave and in the gaseous region outside the cloud if $\beta_0 >> 1$. However if $\beta_0 \approx O(1)$, the quasi-steady assumption will be strictly valid only within the vaporization front.

The quasi-steady analysis of Correa and Sichel showed that T_g^e, and hence the wave speed, increases with the regression of the cloud edge in such a way that the cloud vaporization follows the "D^2 -law", and the cloud life time is given by[6]

$$\bar{t}_c = \frac{\bar{t}_d}{3\varepsilon} = \frac{\beta_0}{2}\frac{1}{ln(1+T_g)}\frac{\bar{R}_0^2}{\bar{\alpha}_0} \qquad (7)$$

For a given initial cloud radius and ambient temperature, the cloud lifetime is therefore linearly proportional to the mass loading ratio β_0. The quasi-steady analysis also leads to a unique saturation condition within the cloud depending on ambient conditions and determined by the relation:

$$\frac{Y_{fs} - Y_{f\infty}}{1 - Y_{fs}} = \frac{\bar{C}p_g(\bar{T}_{g\infty} - \bar{T}_{gs})}{\bar{L}} \qquad (8)$$

This saturation condition is analogous to the wet-bulb state of the corresponding isolated droplet.

On the other hand, for the unsteady case or $\beta_0 \leq O(1)$ it is shown below that the the cloud edge temperature does not increase as rapidly as indicated by the quasi-steady solution. Therefore the "D^2 -law" and the unique saturation condition may no longer remain valid for the droplet cloud. Moreover, if the cloud edge temperature becomes constant, the regression rate of the cloud edge becomes constant too.

The unsteady governing equations for spherical clouds are now formulated below and solved using numerical methods. The unsteady results will then be compared with the above quasi-steady results.

Governing Equations and Numerical Methods

The physical model considered here is a saturated or a dry or "clean" spherical cloud undergoing pure vaporization in an infinite, initially stationary atmosphere. Even though gas motion may be induced by the vaporization, the droplets within the cloud are considered to be stationary. The other major assumptions made to simplify the analysis are: (1) the

droplet interior temperature is uniform, (2) the droplets are initially mono-sized and uniformly dispersed, (3) the droplet surface is in thermodynamic equilibrium with the local ambient, (4) the vaporization and gas motion around individual droplets is quasi-steady, (5) physical properties are constant, (6) Le = 1, (7) the pressure is uniform and constant throughout. The dimensionless governing equations can then be obtained as below using the diffusion time $\bar{R}_0^2/\bar{\alpha}_0$, cloud radius $\bar{R}_0$, and diffusion velocity $\bar{\alpha}_0/\bar{R}_0$ as reference scales.

Gas-Phase (four variables ρ_g, Y_f, T_g, V_r)

$$\frac{\partial \rho_g}{\partial t} + \frac{1}{r^2}\frac{\partial}{\partial r}(\rho_g V_r r^2) = \dot{m} \tag{9}$$

$$\frac{\partial Y_f}{\partial t} + V_r \frac{\partial Y_f}{\partial r} - \frac{1}{\rho_g}\frac{1}{r^2}\frac{\partial}{\partial r}(r^2 \frac{\partial Y_f}{\partial r}) = \frac{\dot{m}}{\rho_g}(1 - Y_f) \tag{10}$$

$$\frac{\partial T_g}{\partial t} + V_r \frac{\partial T_g}{\partial r} - \frac{1}{r_g}\frac{1}{r^2}\frac{\partial}{\partial r}(r^2 \frac{\partial T_g}{\partial r}) = -\frac{\dot{m}}{\rho_g}(Leff + T_g - T_d) \tag{11}$$

$$p = \rho_g (\frac{\bar{T}_{d0}}{\bar{T}_{g0}} + \frac{\bar{L}}{\bar{C}_{pg}\bar{T}_{g0}} T_g)\frac{\bar{W}_0}{\bar{W}} = 1 \tag{12}$$

$$\text{where} \quad \bar{W} = (\frac{Y_f}{\bar{W}_f} + \frac{1 - Y_f}{\bar{W}_a})^{-1} \tag{13}$$

Droplet-Phase (two variables D_d, T_d)

$$\frac{dD_d^2}{dt} = -\frac{2}{3}\frac{1}{\beta_0 \varepsilon} ln(1 + B_Y)\, f(Re) \tag{14}$$

$$\frac{dT_d}{dt} = \frac{\bar{C}_{pg}}{\bar{C}_{pd}}\frac{1}{\beta}\frac{\dot{m}}{\rho_g}(Leff - 1) \tag{15}$$

where $f(Re) = 1 + 0.276\, Re^{1/2}\, Sc^{1/3}$, and Re is the Reynolds number based on the droplet diameter and the relative velocity between the droplet and the gas. The dimensionless vaporization rate $\dot{m}$ in the source terms of the gas equations is given by

$$\dot{m} = \frac{D_d}{\varepsilon} ln(1 + B_Y)\, f(Re) \qquad \text{inside cloud}$$
$$= 0 \qquad \text{outside cloud} \tag{16}$$

in which the mass transfer number B_Y and the dimensionless variable Leff in Eqs. (11) and (15) are defined as

$$B_Y = \frac{Y_{fs} - Y_f}{1 - Y_{fs}}, \qquad Leff = \frac{B_T}{B_Y}, \qquad B_T = T_g - T_d \tag{17}$$

where T_g and Y_f are the local gas temperature and fuel concentration so that the droplet vaporization is computed using the local conditions in the gas surrounding the droplets rather than the far field ambient conditions as used in isolated single droplet vaporization. Tishkoff[9] proposed a correction factor which is greater than one for spray problems using local conditions for individual droplets. However, this correction factor is neglected to simplify the computations and facilitate concentration on the subject of the group vaporization.

The quantity L_{eff} is in fact $\bar{L}_{eff}/\bar{L}$ and $\bar{L}_{eff}$ is an effective latent heat of vaporization which accounts for the heat conducted into the liquid droplet. L_{eff} is generally greater than one and equal to one at the wet-bulb state, and can also be represented by B_T/B_Y[10] as shown in Eq. (17). The saturated fuel concentration Y_{fs} in Eq. (17) is provided by the Clausius-Clapeyron relation as given below.

$$\bar{p}_v = \exp[-\frac{\bar{L}\,\bar{W}_f}{\bar{R}u\,\bar{T}_b}(\frac{\bar{T}_b}{\bar{T}_d} - 1)], \qquad Y_{fs} = [1 + \frac{\bar{W}_a}{\bar{W}_f}(\frac{\bar{p}_\infty}{\bar{p}_v} - 1)]^{-1} \tag{18}$$

The radial velocity V_r in the governing equations cannot be determined directly since the radial momentum equation as shown in Eq. (12) is simply p = 1. The relationship between V_r, Y_f and T_g at a given time is formulated below using the continuity equation and the equation of state making it possible to determine V_r using numerical integration. This procedure follows Polymeropoulos and Peskin[11] who studied the combustion of a stationary vapor cloud. By differentiating the equation of state (12) and using Eq. (13), it follows that

$$d\rho_g = (\frac{\bar{W}}{\bar{W}_a} - \frac{\bar{W}}{\bar{W}_f})\rho_g\, dY_f - \frac{\rho_g}{T_{dg0}/L + T_g}\, dT_g \tag{19}$$

where $T_{dg0} = \bar{T}_{d0}/\bar{T}_{g0}$, $L = \bar{L}/(\bar{C}_{pg}\bar{T}_{g0})$. Writing Eq. (19) in differential form, substituting Eqs. (10) and (11) into Eq. (19) and eliminating the convective terms using the continuity Eq. (9), the resulting equation representing the relationship between V_r, Y_f and T_g at a given time is then given by

$$\frac{1}{r^2}\frac{\partial}{\partial r}(r^2 V_r) = \frac{1}{\rho_g (T_{dg0}/L + T_g)}\frac{1}{r^2}\frac{\partial}{\partial r}(r^2 \frac{\partial T_g}{\partial r}) - \frac{1}{\rho_g}(\frac{\bar{W}}{\bar{W}_a} - \frac{\bar{W}}{\bar{W}_f})\frac{1}{r^2}\frac{\partial}{\partial r}(r^2 \frac{\partial Y_f}{\partial r}) + (\frac{\bar{W}}{\bar{W}_f} - \frac{Leff + T_g - T_d}{T_{dg0}/L + T_g})\frac{\dot{m}}{\rho_g} \tag{20}$$

In actual computations Eq. (20) is used to replace the continuity Eq. (9) as one of the governing equations. Equation (20) contains no derivative with respect to time. As a result, if ρ_g, Y_f, T_g are known at a given time, the corresponding radial velocity V_r can be obtained by the numerical integration of Eq. (20).

The values of various fixed parameters corresponding to an octane fuel and the ambient gas used in the calculations are given in Table 1 below.

Two kinds of initial conditions corresponding to saturated clouds as considered in the quasi-steady analysis [6,7], and to clear or dry clouds with, initially zero fuel vapor concentration are considered below. The initial conditions for initially dry clouds are $\bar{T}_{g\infty} = \bar{T}_{g0} = 1000$ K, $\bar{Y}_{g\infty} = \bar{Y}_{g0} = 0$, $\bar{T}_{d0} = 300$ K or 350 K. For saturated clouds the initial conditions are $T_{g\infty} = 1000$ K,

Table 1 Values of various parameters used in computations

Fuel : Octane		
$\bar{p}_\infty$	Pressure	1 atm
$\bar{\rho}_d$	Liquid droplet density	707 kg/m^3
$\bar{T}_b$	Droplet boiling temperature	398 K
$\bar{L}$	Latent heat of vaporization	71.7 kcal/kg
$\bar{C}_{pd}$	Droplet specific heat	0.52 kcal(kg - K)$^{-1}$
$\bar{C}_{pg}$	Vapor specific heat	0.28 kcal (kg - K)$^{-1}$
$\bar{W}_f$	Fuel molecular weight	114.2 kg (kg - mol)$^{-1}$
$\bar{W}_a$	Air molecular weight	28.9 kg (kg - mol)$^{-1}$

$Y_{f\infty} = 0$, $T_{g0} = 364$ K, $Y_{f0} = 0.707$ which corresponds to the quasi-steady saturated state within the cloud. The base case treated in the numerical computations is that $\varepsilon = 10^{-4}$, $\beta_0 = 1$. The boundary conditions are zero gradients at the center of the cloud and in the far field.

The dimensionless governing equations were solved subject to the above mentioned initial and boundary conditions using an explicit numerical method with a time marching procedure. Similar governing equations have also been solved by Polymeropoulos and Peskin[11], and by Seth et al.[12] At each time step the computational cycle is initiated by solving for Y_f and T_g from the gas equations while r_g is determined from the equation of state. At the same time the droplet properties are determined by solving the droplet equations, and the new values of ρ_g, Y_f, T_g, T_d, D_d are then substituted into Eq. (20) to obtain the updated V_r. The computational cycle is repeated until the droplets in the cloud are completely vaporized or some other specified conditions are met.

The spatial region was discretized into annular cells of uniform width Δr and a centered-difference scheme was applied to the gas equations. The time step size $\Delta t = 10^{-5} - 10^{-6}$ and the spatial cell size $\Delta r = 0.02$ were used for simplicity despite the fact that additional computer time may be required when constant step sizes are used. The computational domain is $r \leq 5$ when $b_0 = 1$ and $r \leq 10$ when $b_0 = 5$ in order to provide complete coverage of the region where gas diffusion occurs during cloud vaporization.

Numerical Results and Comparisons

Figure 2 shows the variation of dimensionless droplet size with radius at various times for saturated clouds with $\beta_0 = 1$ and $\varepsilon = 10^{-4}$. The droplet size within the cloud remains essentially unchanged. The droplet size drops steeply at the cloud edge so that the thickness of the vaporization layer can be clearly identified. This thickness seems to remain constant during the cloud lifetime. It can be seen that the vaporization wave moves into the cloud rapidly during a transient period, then appears to move at a constant speed during an intermediate period, and then accelerates during a final period just before vaporization is complete.

Figures 3 and 4 show the profiles of the dimensionless temperature T_g and fuel concentration Y_f at various times. It can be seen that while the high temperature region diffuses toward the cloud, and the fuel diffuses outward, the conditions within the cloud, i.e., inside the vaporization wave remain unchanged.

Figure 5 shows the profiles of the gas radial velocity V_r at various times. Within the vaporization layer, which can be seen clearly in the figure, V_r increases from zero to a peak which is taken as the location of the cloud edge. Beyond the cloud edge V_r, either increases or decreases, first reaches a local maximum or minimum value, and then decreases to a negative minimum value, and then gradually approaches the value of zero. It can also be seen that the position of $V_r = 0$ moves away from the cloud as time increases.

The above profiles of the radial velocity depend on the specific liquid fuel properties and are also a consequence the imposed initial jump conditions. The cloud interior is initially a region of low-temperature and high fuel concentration. The outward diffusion of fuel vapor tends to decrease the pressure within the cloud, while the inward diffusion of heat from the ambience tends to increase the pressure within the cloud. Due to its high molecular weight $\bar{W}_f$, the outward diffusion of fuel vapor dominates and hence induces a flow toward the cloud in the ambient gas. However, near the cloud edge droplet vaporization still favors a positive radial velocity. V_r is therefore positive near the cloud edge and becomes negative in the region away from the cloud. As the cloud continues to vaporize the fuel vapor continues to diffuse away from the cloud and heat continues to diffuse inward causing the region of positive V_r to expand so that the position of $V_r = 0$ moves away from the cloud.

Figures 6 and 7 show the variation of the dimensionless cloud radius R and the square of cloud radius R^2 with time for $\beta_0 = 0.1$, 1, 5. The zigzag contours in these figures are due to the spatial discretization of the finite difference scheme. It can be seen that unsteady cloud vaporization more closely follows a "D - law" rather than a "D^2 - law" unless $\beta_0 >> 1$, while the quasi-steady analysis as adopted by Correa and Sichel[6,7] will only lead to the "D^2 - law". It can also be seen that the regression speed of the vaporization wave is a function of β_0 so that the cloud life time is also a function of β_0 since it is determined by the regression of the wave.

Figure 8 shows the variation of the dimensionless cloud lifetime τ_c with the droplet loading ratio

β_0. The results of the quasi-steady theory of Correa and Sichel[6] as given by Eq. (7) match well with the unsteady numerical solutions for $\beta_0 > 1$ due to the presence of the thin vaporization wave, but under-estimate the cloud lifetime for $\beta_0 < 1$ due to the over-estimate of the cloud edge temperature.

Figures 9 - 11 are the results for the initially dry droplet clouds with $\beta_0 = 5$. It can be seen from Fig. 9 that the cloud interior reaches the saturated state in a very short time compared to the cloud lifetime. Figure 10 shows the induced gas radial velocity which assumes very large negative values as soon as $t > 0$. The immediate appearance of the large V_r is due to the use of the "D^2 - law" for droplet vaporization, and may be modified by using the "diffusion-limit model" (i.e., non-uniform droplet interior temperature) for single droplet vaporization as used by Aggarwal et al.[13] According to the "D^2-law" vaporization starts instantaneously at $t = 0$ in the dry cloud and thus accounts for the sudden and physically unrealistic appearance of a radial velocity component. The actual magnitude of V_r will not be very large and will decrease significantly after an initial transient period. The negative value of V_r is due to the dominance of evaporative cooling and the specific liquid fuel properties. This effect can be seen from Eq. (20) where it is evident that a high latent heat of vaporization $\bar{L}$ and a high molecular weight $\bar{W}_f$ cause the third term on the right hand side to be negative. The local maxima around the position $r = 1$ are due to the fact that the droplet vaporization rate at the cloud edge is higher than that within the cloud.

Figure 11 shows the variation of the saturation temperature within the cloud for various values of the initial ambient temperature. For the initially dry cloud there is no sheath layer at the cloud edge to justify the quasi-steady analysis. The saturation temperature is then not uniquely determined by Eq. (8) but depends on both $\bar{T}_{g0}$ and $\bar{T}_{d0}$. The quasi-steady saturation temperature generally cannot be achieved within the cloud unless $\bar{T}_{d0}$ is initially greater than the wet-bulb temperature of the corresponding isolated droplet. The quasi-steady saturation temperature within the cloud is in fact the wet-bulb temperature for the corresponding isolated droplet. It should also be noted that there is a sharp increase in the saturation temperature when the initial gas temperature is very high. The temperature on this portion of the curve is actually not the saturation temperature but the temperature at which the cloud vaporizes completely.

Discussion and Conclusions

The quasi-steady and unsteady vaporization of spherical fuel droplet clouds has been discussed in this study. Previous theoretical studies[14,15] have shown that the vaporization of a liquid droplet near the critical state (or at high pressures) is inherently unsteady in nature due to the like order of magnitude of the densities of the droplet and the surrounding gas. It is therefore not surprising that the vaporization of droplet clouds should also be unsteady. However, the vaporization of saturated clouds (for $\varepsilon << 1$) has a distinctive nature in that a vaporization layer existing at the cloud edge will block the transfer of heat from the ambient into the cloud interior. The characteristic length scale which determines the cloud edge temperature is then the thickness of the vaporization layer rather the cloud radius. The cloud edge temperature in turn determines the propagation speed of the vaporization layer, and hence the cloud lifetime.

The quasi-steady analysis of cloud vaporization is justified if the following conditions are met: (i) $\beta_0 \geq O(1)$, (ii) the existence of the thin vaporization layer at the cloud edge. If the first condition $\beta_0 \geq O(1)$ is not satisfied, then even though a vaporization layer at the cloud edge may exist, the quasi-steady approximation becomes invalid due to the fact that the diffusion velocity is no greater than the vaporization wave velocity. As a result of this the cloud vaporization is found to follow a "D - law" rather than the classical "D^2 -law" for single droplet vaporization. The quasi-steady theory then under-estimates the cloud life time due to the over-estimate of the temperature at the cloud edge. The second condition, that there is a vaporization layer, is not met when the droplets start to vaporize in an initially dry cloud. As a result, the saturation temperature within the cloud is no longer uniquely determined but depends on both $\bar{T}_{g\infty}$ and $\bar{T}_{d0}$. The saturation temperature, which is found in the quasi steady analysis is actually the wet-bulb temperature for a corresponding isolated droplet. If conditions (i) and (ii) above are satisfied, the quasi-steady theory is valid in a narrow region $\bar{R} < \bar{r} < \bar{R} + O(\bar{\delta})$ and provides an excellent prediction of the cloud lifetime implying that the overall heat transfer to the cloud surface is the same for both the quasi-steady and unsteady analyses. The processes in the ambient gas greater than a distance of $O(\bar{\delta})$ from the cloud remain unsteady. This situation is analogous to single droplet vaporization where the processes involved are unsteady in the far field.

NOMENCLATURE

Dimensional Variables

$\bar{C}_p$	specific heat
$\bar{D}_d$	droplet diameter
$\bar{L}$	latent heat of vaporization
$\bar{L}_{eff}$	$= \bar{L} + \bar{m}_d \bar{C}_{p_d}$
$(d\bar{T}_d/d\bar{t})/\dot{m}_d$	effective latent heat
$\bar{m}_d$	single droplet mass
$\bar{n}$	droplet number density
$\dot{m}_d$	vaporization rate per droplet
$\bar{p}$	pressure
$\bar{R}$	cloud radius
$\bar{R}_u$	universal gas constant
$\bar{r}$	radial coordinate
$\bar{t}$	time
$\bar{T}$	temperature
$\bar{U}_w$	vaporization wave velocity
$\bar{V}_r$	gas radial velocity
$\bar{W}$	molecular weight
$\bar{a}$	thermal diffusivity
$\bar{\delta}$	thickness of the vaporization layer
$\bar{\lambda}$	thermal conductivity
$\bar{\rho}$	density

$\bar{\tau}_c$	cloud life time
$\bar{\tau}_d$	single droplet life time

Dimensionless Variables

B_T	$= T_g - T_d$, heat transfer number
B_Y	$= (Y_{fs} - Y_f)/(1 - Y_{fs})$, mass transfer number
D_d	$= \bar{D}_d / \bar{D}_{d0}$
G	$= 2p\,\bar{n}_0 \bar{D}_{d0} \bar{R}_0^2$, group combustion number
L	$= \bar{L}/(\bar{C}p_g \bar{T}_{g0})$
Leff	$= \bar{L}eff/\bar{L}$ $(= B_T/B_Y)$
Le	Lewis number
$\dot{m}$	$= \dot{\bar{m}}_d \bar{n}_0 (\bar{R}_0^2/\bar{\alpha}_0)/\bar{\rho}_{g0}$
p	$= \bar{p}/\bar{p}_\infty = 1$
R	$= \bar{R}/\bar{R}_0$
Re	Reynolds number
r	$= \bar{r}/\bar{R}_0$
T	$= \bar{C}p_g(\bar{T} - \bar{T}_{d0})/\bar{L}$
T_{dg0}	$= \bar{T}_{d0}/\bar{T}_{g0}$
t	$= \bar{t}/(\bar{R}_0^2/\bar{\alpha}_0)$
V_r	$= \bar{V}_r/(\bar{\alpha}_0/\bar{R}_0)$
Y	fuel concentration
β	$= \frac{1}{6}\pi \bar{n} \bar{\rho}_d \bar{D}_d^3/\bar{\rho}_g$, droplet mass loading ratio
ε	$= (2\pi \bar{n}_0 \bar{D}_{d0} \bar{R}_0^2)^{-1}$
ρ_g	$= \bar{\rho}_g/\bar{\rho}_{g0}$
τ_c	$= \bar{\tau}_c/(\bar{R}_0^2/\bar{\alpha}_0)$

Subscripts

0	initial condition inside the cloud
a	air
b	boiling condition
c	cloud
d	droplet
f	fuel
g	gas
r	radial direction
s	saturated condition
w	vaporization wave
∞	ambient condition

Superscripts

e	cloud edge
$(\bar{\ })$	dimensional quantity

REFERENCES

1. Chigier, N. A., and McCreath, C. G., "Combustion of Droplets in Sprays," *Acta Astronautica*, 1, 1974, pp. 687-710.
2. Onuma,Y., and Ogasawara, M., "Studies on the Structure of a Spray Combustion Flame," *Fifteenth Symposium (International) on Combustion*, The Combustion Institute, 1974, pp. 453-465.
3. Chiu, H.H., and Liu, T.M., "Group Combustion of Liquid Droplets," *Combustion Science and Technology*, 17, 1977, pp. 127-142.
4. Annamalai, K., and Ramalingam, S.C., "Group Combustion of Char/Carbon Particles," *Combustion and Flame*, 70, 1987, pp. 307-332.
5. Zhuang, F. C., Yang, B., Zhou, J., and Yang, H., "Unsteady Combustion and Vaporization of a Spherical Fuel Droplet Group," *Twenty-first Symposium (International) on Combustion*,, The Combustion Institute, 1986, pp. 647-653.
6. Correa, S.M., and Sichel, M., "The Boundary Layer Structure of a Vaporizing Fuel Cloud," *Combustion Science and Technology*, 28, 1982, pp. 121-130
7. Correa, S M., and Sichel, M., "The Group Combustion of a Spherical Cloud of Monodisperse Fuel Droplets," *Nineteenth Symposium (International) on Combustion*, 1982, pp. 981-991.
8. Suzuki, T., and Chiu, H.H., "Multi-droplet Combustion of Liquid Propellants,", *Proceedings. of Ninth (International) Symposium on Space Technology and Science.*, Tokyo, Japan, 1971, pp. 145-154.
9. Tishkoff, J. M., "A Model for the effect of Droplet Interactions on Vaporization," *Int. J. Heat Mass Transfer*, 22, 1979, pp. 1407-1415.
10. Faeth, G. M., "Current Status of Droplet and Liquid Combustion," *Progresses in Energy and Combustion Science.*, 3, 1977, pp. 191-224.
11. Polymeropoulos, C. E., and Peskin, R. L. , "Combustion of Fuel Vapor in a Hot, Stagnant Oxidizing Environment," *Combustion Science and Technology*, 5, 1972, pp. 165-174.
12. Seth, B., Aggarwal, S. K., and Sirignano, W. A. , "Flame Propagation Through an Air-Fuel Spray Mixture with Transient Droplet Vaporization," *Combustion and Flame*, 39, 1980, pp. 149-168.
13. Aggarwal, S. K., Tong, A. Y. and Sirignano, W. A., "A Comparison of Vaporization Models in Spray Calculations," *AIAA J.*, 22, 10, 1984, pp. 1448-1457.
14. Spalding, D. B., "Theory of Particle Combustion at High Pressures," *ARS J.*, 29, 1959, pp. 828-835.
15. Rosner, D. E. and Chang, W. S., "Transient Evaporization and Combustion of a Fuel Droplet near its Critical Temperature," *Combustion Science and Technology*, 7, 1973, pp. 145-158.

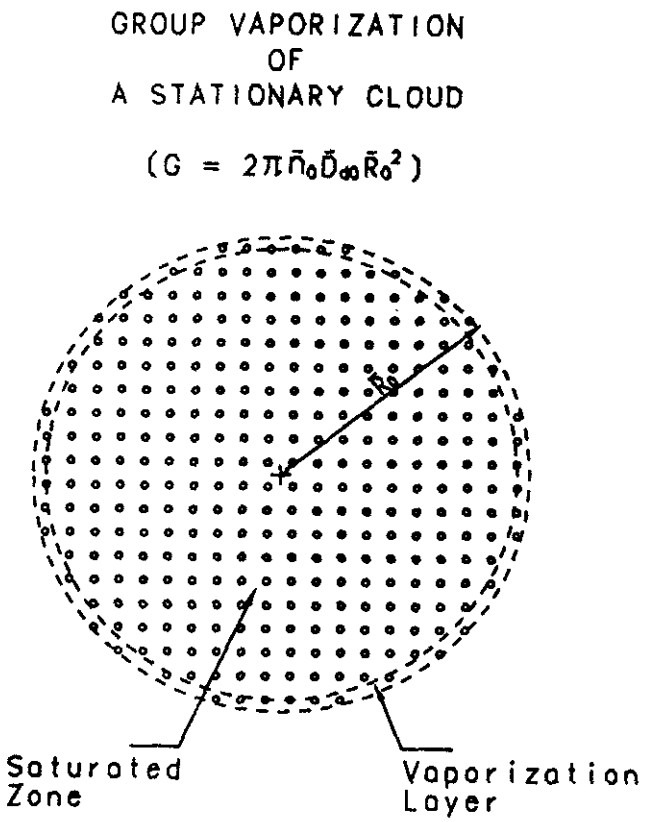

Figure 1 Physical picture of group vaporization of a droplet cloud in a stationary atmosphere

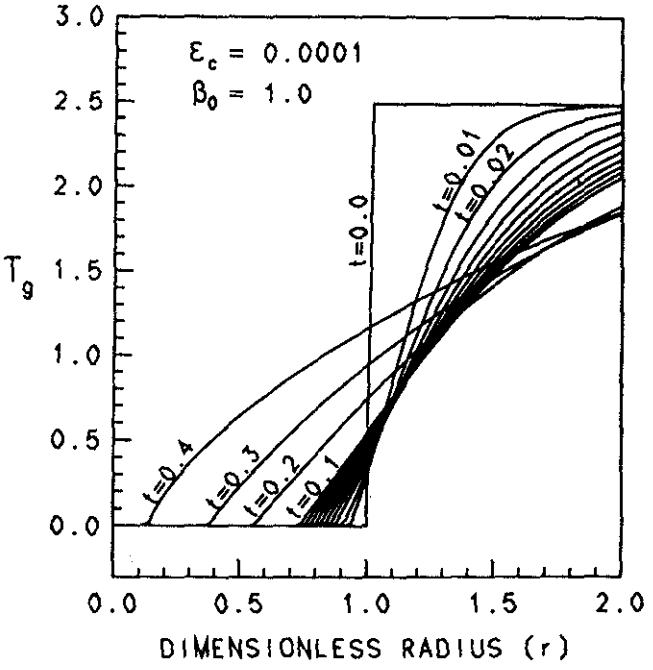

Figure 3 Profiles of dimensionless gas temperature at various times for saturated clouds

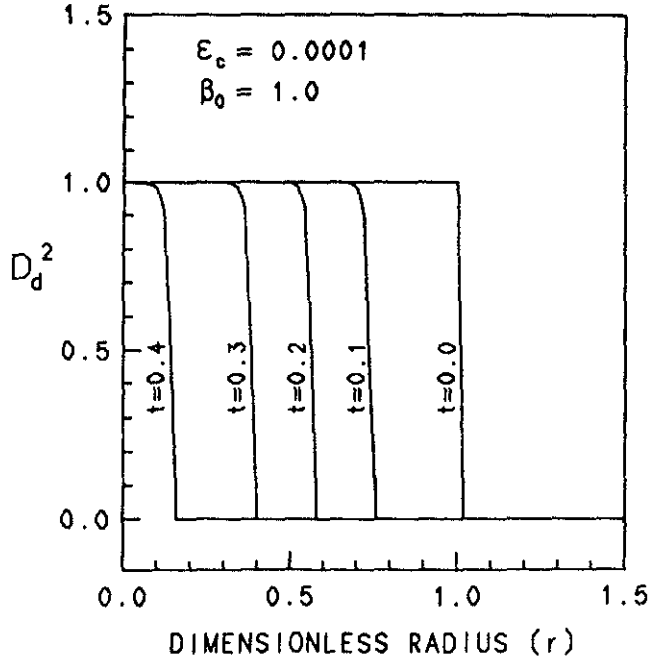

Figure 2 Profiles of dimensionless droplet size at various times for saturated clouds

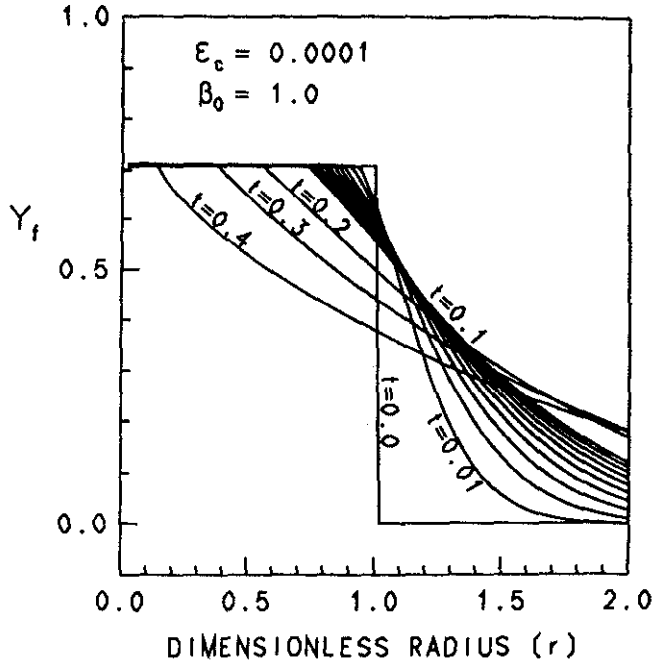

Figure 4 Profiles of fuel concentration at various times for saturated clouds

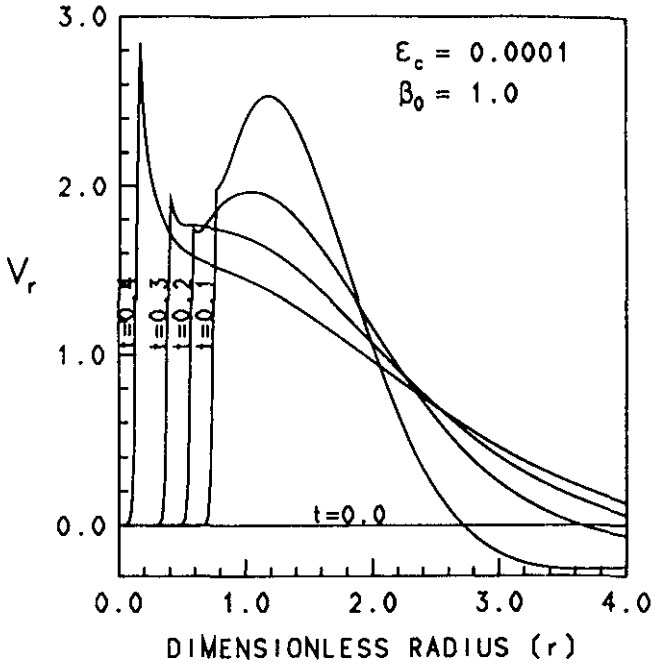

Figure 5 Profiles of dimensionless gas radial velocity at various times for saturated clouds

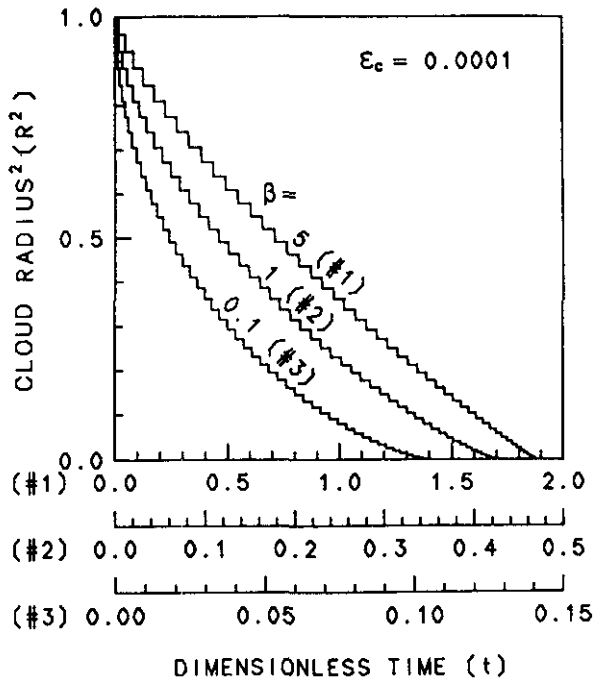

Figure 7 Variation of R^2 with time for saturated clouds

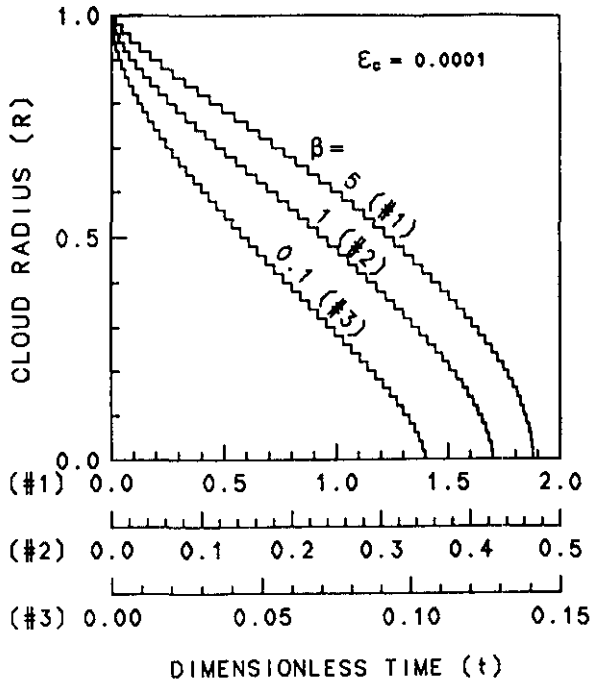

Figure 6 Variation of dimensionless cloud radius R with time for saturated clouds

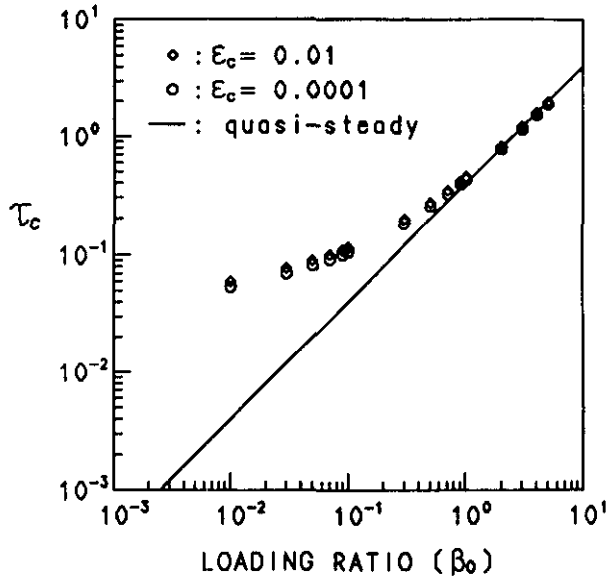

Figure 8 Comparisons between quasi-steady and numerical solutions of τ_c versus β_0 for saturated clouds

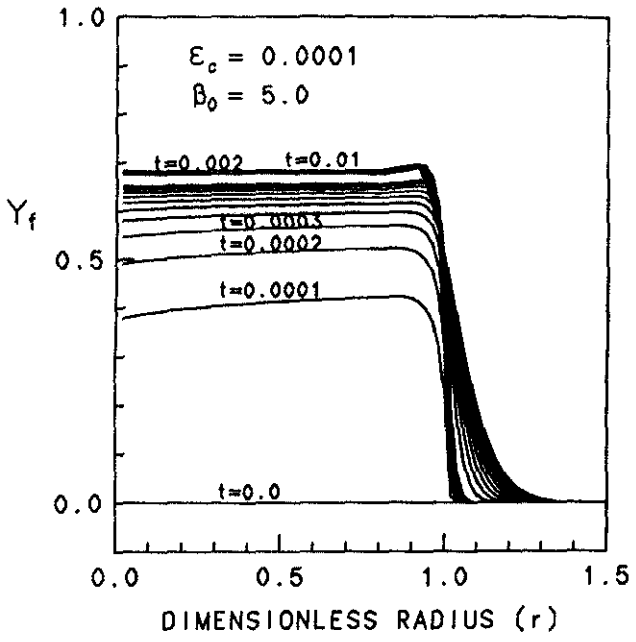

Figure 9 Profiles of fuel concentration at various times for initially clean clouds

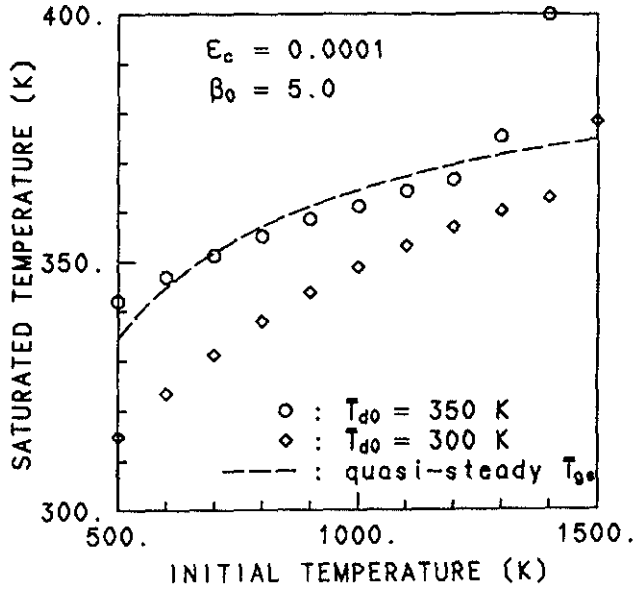

Figure 11 Saturated cloud temperature for initially clean clouds versus initial ambient temperatures

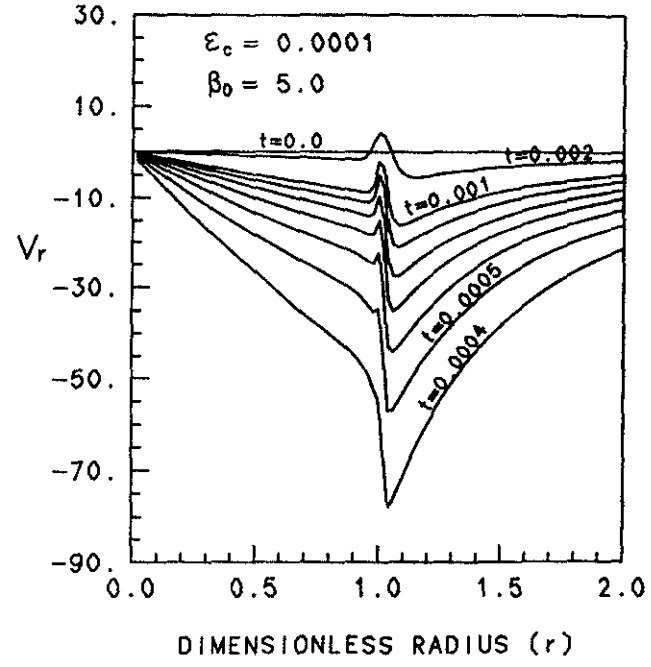

Figure 10 Profiles of dimensionless gas radial velocity at various times for initially clean clouds